

A statistical model for cladding diameter of optical fibres

C M Wang and Timothy J Drapela

National Institute of Standards and Technology, Boulder, CO 80305, USA

E-mail: jwang@boulder.nist.gov

Received 27 August 2002

Published 1 April 2003

Online at stacks.iop.org/Met/40/57

Abstract

The National Institute of Standards and Technology has developed a contact micrometer for accurate measurement of the outer diameter of optical fibres. The contact micrometer is used to measure reference fibres that are artefacts used by the telecommunications industry for calibrating their own measurement systems. We present a model for diameters measured by the contact micrometer. Based on this model, the probability distribution of the diameters is derived and two diameter estimates are presented. We illustrate and compare the diameter estimates using simulated data.

1. Introduction

The optical fibre industry has developed the grey-scale method [1], which uses a video microscope for measuring the geometrical parameters of the cleaved end of a telecommunications fibre. A typical single-mode optical fibre is nearly circular and has a glass core of about $10\ \mu\text{m}$ in diameter surrounded by a glass cladding with an outer diameter of about $125\ \mu\text{m}$. Grey-scale systems are used to determine the cladding diameter, the non-circularity of the cladding, and the decentring, or concentricity error, between the core and the cladding. Measurements of non-circularity and decentring do not require high absolute accuracy. The cladding diameter, however, must be measured and controlled within $0.1\ \mu\text{m}$ to enable the manufacture of efficient fibre connectors that do not require manual adjustment.

Measurements made with grey-scale systems may suffer from a systematic error of a few tenths of a micrometre [2]. Consequently, industry needs a standard so that they can correct for this systematic error. The National Institute of Standards and Technology (NIST) has developed a contact micrometer that can make cladding-diameter measurements accurate to $0.04\ \mu\text{m}$ [3]. The contact micrometer is used to certify standard reference material (SRM) fibres that have been commercially available since 1993.

Each SRM is individually calibrated. The SRM consists of a short length of fibre in an aluminium housing. Cladding diameters of the reference fibre are measured (by the contact micrometer) at angular orientations of 0° , 45° , 90° , and 135° , and the results are listed in an accompanying certificate. The positions of these angles are marked by radial lines scribed at the rear of the housing. To calibrate the grey-scale or other

systems, the user simply follows the instructions described in the certificate to place the housing in the system at one of the four angular positions, measures the diameter of the reference fibre, compares it with the certified diameter, and calibrates the system accordingly.

The above calibration procedure requires that the reference fibre be contained in a housing that has lines scribed at 45° intervals. In some special cases, NIST is asked to provide calibration service for measurement systems that have their own holders. In these cases, after diameter measurements are taken, the NIST reference fibre is removed from its housing and mounted into the alternative holder. In transferring the fibre, the identification of angular orientation may be lost. If the transverse diameter is measured by the system (which is more like the NIST contact micrometer than a grey-scale system) to be calibrated, the measurements may be limited to comparison with a single certified value of diameter because of the lack of angular information. Consequently, we need to report a certified diameter for the reference fibre so it can be compared with the diameter obtained from a measurement system having the fibre oriented at any angle.

In this article, we propose a model for diameters measured by the contact micrometer. Based on this model, the probability distribution of the diameters is derived. Two diameter estimates are presented. The first estimate is based on the mean of the diameter measurements at equally spaced angular orientations. The second estimate is obtained from a non-linear estimation of elliptical parameters of the model. The standard errors of the estimates for various sampling schemes are calculated. We illustrate and compare the diameter estimates using simulated data.

2. Model of fibre cross section

Because fibre-cladding non-circularity is one of the primary geometric measurements of interest, an ellipse rather than a circle is used to model the cross section of a fibre. To be consistent with formulations used in the industry, we express the equation of the ellipse (assuming that it does not pass through the origin) as

$$f(x, y) = Ax^2 + Bxy + Cy^2 + Dx + Ey + 1 = 0, \quad (1)$$

where $B^2 - 4AC < 0$. The centre of the ellipse is located at (α, β) , where

$$\alpha = \frac{2CD - BE}{B^2 - 4AC}, \quad (2)$$

$$\beta = \frac{2AE - BD}{B^2 - 4AC} \quad (3)$$

and the major axis makes an angle of

$$\theta = \frac{1}{2} \tan^{-1} \left(\frac{B}{A - C} \right) \quad (4)$$

with the positive x -axis. The length of the semi-major axis, M , is the larger of

$$\sqrt{\frac{2(\alpha^2 A + \alpha\beta B + \beta^2 C - 1)}{A + C + (B/\sin 2\theta)}} \quad (5)$$

and

$$\sqrt{\frac{2(\alpha^2 A + \alpha\beta B + \beta^2 C - 1)}{A + C - (B/\sin 2\theta)}}, \quad (6)$$

depending on the sign of $B/\sin 2\theta$, and the length of the semi-minor axis, m , is the smaller. In fibre modelling, the mean diameter of the ellipse is defined to be the sum $M + m$, while the non-circularity δ is defined as $(M - m)/(M + m)$ and is expressed as a percentage. The mean diameter and non-circularity are estimated by substituting appropriate parameter estimates $\hat{A}, \hat{B}, \hat{C}, \hat{D}, \hat{E}$ in (2)–(6). Both the ordinary least squares and errors-in-variables [4], or orthogonal-distance least squares, can be used to fit (1) to grey-scale images. For a detailed discussion on statistical methods applied to the estimation of optical-fibre geometry, see [5, 6].

3. Contact micrometer

A contact micrometer [7] consists of a stationary post called an anvil, and a movable part called a spindle. Measurements are performed by first pressing the fibre between the spindle and the anvil, with the position of the spindle being monitored interferometrically. Then, the fibre is removed, and the spindle is brought into contact with the anvil. The difference between the two positions is the diameter of the fibre. If we model the cross section of the fibre by an ellipse, then the contact micrometer measures the horizontal width of the ellipse as the diameter of the fibre. Figure 1 shows the horizontal width \overline{AB} of an ellipse.

The width in figure 1 is determined by the x -coordinates of the two vertical tangent lines of the ellipse. From (1), we find that

$$\frac{dy}{dx} = \frac{-B}{2C} \pm \frac{(B^2 x + BE)/2C - 2AX - D}{G},$$

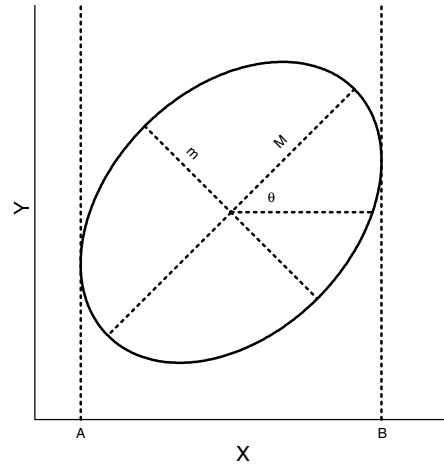


Figure 1. The horizontal width (\overline{AB}) of an ellipse.

where

$$G = \sqrt{\left(\frac{B^2}{4} - AC\right)x^2 - \left(CD - \frac{BE}{2}\right)x + \frac{E^2}{4} - C}.$$

The values of x such that $dy/dx = \pm\infty$ satisfy $G = 0$, or

$$x = \frac{BE - 2CD}{4AC - B^2} \mp \frac{\sqrt{(BE - 2CD)^2 - (4AC - B^2)(4C - E^2)}}{4AC - B^2}. \quad (7)$$

After some algebra, (7) reduces to

$$x = \alpha \mp \sqrt{m^2 \sin^2 \theta + M^2 \cos^2 \theta}.$$

Thus,

$$W = \overline{AB} = 2\sqrt{m^2 \sin^2 \theta + M^2 \cos^2 \theta}. \quad (8)$$

For given M and m , the horizontal width W depends on the orientation of the ellipse. Since θ can take any value between 0 and 2π , we can obtain the probability density function (pdf) of W by assuming that θ is distributed uniformly in $[0, 2\pi]$. Based on this assumption, the pdf of W is found to be

$$f_W(w) = \frac{w}{\pi \sqrt{(M^2 - m^2)^2 - (w^2/2 - M^2 - m^2)^2}} \quad 2m < w < 2M. \quad (9)$$

Figure 2 displays a histogram of W obtained from 100 000 simulated values of θ with $M = 63$ and $m = 62$. The superimposed line is the pdf of W . The tails of this U-shaped pdf play a significant role in the estimation of the cladding diameter, which is discussed in the next section.

4. Estimation of diameter with exact angular control

The first method for estimating the cladding diameter based on measurements from a contact micrometer uses measurements at equally spaced angular orientations. Specifically, we use the mean of horizontal widths at angles of $0^\circ, 45^\circ, 9^\circ,$ and 135° to estimate the diameter. A plausible model for these measurements is

$$w_i = 2\sqrt{m^2 \sin^2(u_i - \theta_0) + M^2 \cos^2(u_i - \theta_0)} + \epsilon_i = W_i + \epsilon_i, \quad (10)$$

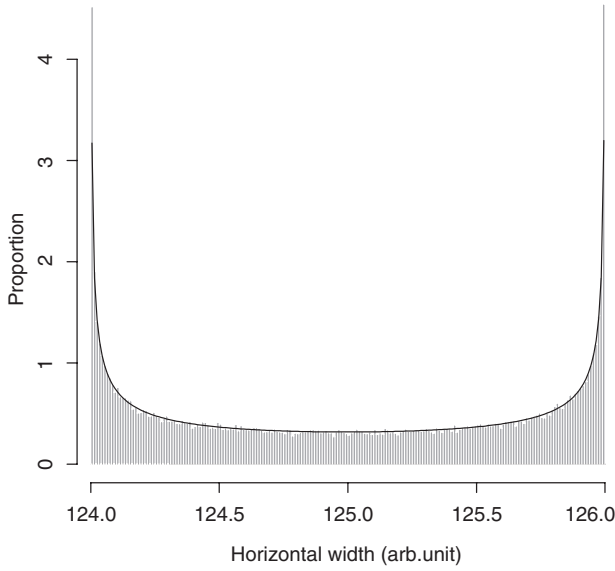


Figure 2. Histogram and pdf of horizontal widths of an ellipse with $M = 63$ and $m = 62$.

where $u_i = (i-1)\pi/4$, $i = 1, 2, 3, 4$, θ_0 is the unknown initial orientation of the ellipse, and ϵ_i are the zero-mean random noise with standard deviation σ_ϵ . In a typical measurement, σ_ϵ is estimated to be $0.014 \mu\text{m}$ [3]. Note that the W_i are identically distributed but are correlated.

To simplify the presentation, we work with the standardized horizontal width

$$V_i = \frac{W_i}{M+m} = 2\sqrt{\rho^2 \sin^2(u_i - \theta_0) + (1-\rho)^2 \cos^2(u_i - \theta_0)},$$

where $\rho = m/(M+m)$, to evaluate the mean and variance of the diameter estimator $\bar{w}_4 = \sum_{i=1}^4 w_i/4$.

We first evaluate $E(V_i)$. It is seen that

$$E(V_i) = \frac{1}{2\pi} \int_0^{2\pi} 2\sqrt{\rho^2 \sin^2 \theta + (1-\rho)^2 \cos^2 \theta} d\theta. \quad (11)$$

The above integral is an elliptic integral of the second kind [8] and can be evaluated accurately. Expanding the integrand about $\rho = 1/2$, dropping all terms of order higher than six, and then integrating, we obtain the approximation

$$E(V_i) \approx 1 + \left(\rho - \frac{1}{2}\right)^2 + \frac{1}{4} \left(\rho - \frac{1}{2}\right)^4 + \frac{1}{4} \left(\rho - \frac{1}{2}\right)^6. \quad (12)$$

For values of ρ that are relevant to our applications ($\delta < 1\%$), the absolute difference between the exact and approximate $E(V_i)$ is smaller than 10^{-17} . Even if δ is as large as 2%, the absolute difference is still smaller than 10^{-8} . Thus, we use

$$E(\bar{w}_4) \approx (M+m) \left(1 + \frac{\delta^2}{2^2} + \frac{\delta^4}{2^6} + \frac{\delta^6}{2^8}\right). \quad (13)$$

Recall that δ is the non-circularity measure.

To evaluate $\text{var}(\bar{w}_4)$, we need to evaluate the covariances of V_i and V_j . It is seen that $\text{cov}(V_i, V_j)$ depends only on $|u_i - u_j|$. That is, $\text{cov}(V_1, V_2) = \text{cov}(V_2, V_3) = \text{cov}(V_3, V_4)$, and $\text{cov}(V_1, V_3) = \text{cov}(V_2, V_4)$. Also, since V_i is periodic

with period $= \pi$, $\text{cov}(V_1, V_4) = \text{cov}(V_1, V_2)$. In other words, we need only to evaluate $E(V_1^2)$, $E(V_1 V_2)$, and $E(V_1 V_3)$. For $E(V_1^2)$, we can obtain the exact result with

$$\begin{aligned} E(V_1^2) &= \frac{1}{2\pi} \int_0^{2\pi} 4(\rho^2 \sin^2 \theta + (1-\rho)^2 \cos^2 \theta) d\theta \\ &= 2\rho^2 + 2(1-\rho)^2, \end{aligned}$$

We use the Taylor expansion to obtain the approximations

$$E(V_1 V_2) \approx 1 + 2\left(\rho - \frac{1}{2}\right)^2 + \left(\rho - \frac{1}{2}\right)^4 + 2\left(\rho - \frac{1}{2}\right)^6$$

and

$$E(V_1 V_3) \approx 1 + 4\left(\rho - \frac{1}{2}\right)^4 + 4\left(\rho - \frac{1}{2}\right)^8.$$

Again, the exact and approximate results of $E(V_1 V_2)$ and $E(V_1 V_3)$ are practically equal, even if δ is as large as 2%. Based on these results, it can be shown that

$$\begin{aligned} \text{var}(\bar{w}_4) &= \frac{1}{4} \text{var}(W_1) + \frac{1}{2} \text{cov}(W_1, W_2) \\ &\quad + \frac{1}{4} \text{cov}(W_1, W_3) + \frac{1}{4} \sigma_\epsilon^2 \\ &\approx \frac{7}{2^{12}} (M+m)^2 \delta^8 + \frac{1}{4} \sigma_\epsilon^2. \end{aligned} \quad (14)$$

The first term on the right-hand side of (14) is due to the variation of the means of the four horizontal widths, and the second term is due to the measurement errors. The first term is much smaller than the second term even when the non-circularity is moderate. For example, when $M = 63 \mu\text{m}$ and $m = 62 \mu\text{m}$,

$$\text{var}(\bar{w}_4) \approx 0.448 \times 10^{-15} \mu\text{m}^2 + 0.49 \times 10^{-4} \mu\text{m}^2.$$

Thus, only the measurement errors contribute to the overall uncertainty of \bar{w}_4 and hence \bar{w}_4 is an adequate estimator of the diameter.

For $u_i = (i-1)\pi/4$, $i = 1, 2, \dots, 8$, we have $W_j = W_{j+4}$, $j = 1, 2, 3, 4$, and $\sum_{i=1}^8 W_i/8 = \sum_{i=1}^4 W_i/4$. That is, \bar{w}_4 is essentially a mean of measurements at equally spaced angles around a circle. Diameter estimators based on measurements from other sampling schemes produce larger uncertainties than that produced by \bar{w}_4 . For the extreme case, let \bar{w}_r be the mean of four measurements at random angular orientations. Then,

$$\begin{aligned} \text{var}(\bar{w}_r) &= \frac{1}{4} \text{var}(W_1) + \frac{1}{4} \sigma_\epsilon^2 \\ &\approx 0.125 \mu\text{m}^2 + 0.49 \times 10^{-4} \mu\text{m}^2 \end{aligned} \quad (15)$$

for $M = 63 \mu\text{m}$ and $m = 62 \mu\text{m}$. Obviously, the uncertainty of \bar{w}_r is too large to be acceptable. Also, let \bar{w}_7 be the mean of seven measurements at angles of $(i-1)\pi/4$, $i = 1, 2, \dots, 7$, i.e. angles are equally spaced but do not complete the circle. Then,

$$\begin{aligned} \text{var}(\bar{w}_7) &= \frac{13}{49} \text{var}(W_1) + \frac{24}{49} \text{cov}(W_1, W_2) \\ &\quad + \frac{12}{49} \text{cov}(W_1, W_3) + \frac{1}{7} \sigma_\epsilon^2 \\ &\approx \frac{7}{2^{12}} (M+m)^2 \delta^8 + \frac{1}{98} (M+m)^2 \delta^2 + \frac{1}{7} \sigma_\epsilon^2. \end{aligned} \quad (16)$$

Comparing (16) with (14), $\text{var}(\bar{w}_7)$ has an extra term in δ^2 . This term can be relatively large if the non-circularity is not

small. For example, when $M = 63 \mu\text{m}$ and $m = 62 \mu\text{m}$, this term is $0.0102 \mu\text{m}^2$, which is much larger than the error term of $0.28 \times 10^{-4} \mu\text{m}^2$. Thus, \bar{w}_7 is an inferior diameter estimator to \bar{w}_4 even though three more measurements were used. This is because the sampling scheme corresponding to \bar{w}_7 produces uneven numbers of horizontal width measurements in the tail areas (see figure 2). Depending on the initial orientation of the fibre, either two measurements are taken in the left tail (three in the right tail) or three measurements in the left tail (two in the right tail), resulting in a mean having a larger variance than the mean based on a balanced scheme. A similar result on the optimality of balanced sampling schemes for measurements collected on the circumference of circular features was discussed in [9].

5. Estimation of diameter with known angular increment

The second method of estimating fibre diameter by means of contact micrometer measurements is based on known angular increments. Sometimes, it may not be possible to rotate the fibre to a desired orientation with acceptable precision. Instead, it can be rotated by a fixed mechanism, which corresponds to a known angular increment. That is, the resulting sampling scheme may not be balanced. Since the increments are known, based on (u_i, w_i) , we can first estimate the parameters m, M , and θ_0 in (10) using non-linear regression and then use these parameter estimates to determine the expected horizontal width according to (13). However, since for a typical fibre, the $(M + m)\delta^2/4$ term in (13) is smaller than the last digit of the value used in reporting the certified diameter, and in order to be consistent with the grey-scale method, we estimate the diameter using \hat{W} with

$$\hat{W} = \hat{M} + \hat{m}, \tag{17}$$

where \hat{M} and \hat{m} are obtained from the non-linear fit of (10). Although sampling plans are critical to the optimality of non-linear parameter estimates \hat{M} and \hat{m} , and hence \hat{W} , we can compensate for the lack of balanced sampling schemes by increasing the number of measurements used in the non-linear fit. Thus, the effects of an unbalanced sampling scheme should be less drastic than what we observed in the previous section for means of w_i .

The variance of \hat{W} is approximated by

$$\text{var}(\hat{W}) \approx \text{var}(\hat{M}) + \text{var}(\hat{m}) + 2\text{cov}(\hat{M}, \hat{m}), \tag{18}$$

where the variance and covariance of \hat{W} and \hat{m} are part of the non-linear least-squares solution. We use simulations to illustrate the method proposed in this section.

The units of the fibre diameter used in the simulation are micrometres. The first simulation is based on the seven-measurement example in the last section. We first generate $w_i, i = 1, 2, \dots, 7$, according to (10) with $(M, m) = (63, 62)$ and $(M, m) = (63.75, 61.25)$, $u_i = (i - 1)\pi/4$, and an arbitrary orientation θ_0 . Gaussian random noises with mean 0 and standard deviation 0.014 are used to perturb the measurements. We then obtain the least-squares estimates of M, m , and θ_0 based on $(u_i, w_i), i = 1, 2, \dots, 7$. We also obtain the diameter estimator \hat{W} of (17), its estimated variance of (18),

Table 1. Simulation results (μm) for $u_i = (i - 1)45^\circ, i = 1, 2, \dots, 7$.

	$M = 63, m = 62$		$M = 63.75, m = 61.25$	
	Mean	Sd	Mean	Sd
\hat{W}	125.000	0.005 40	125.012	0.005 40
\bar{w}_7	125.000	0.101 70	125.008	0.253 90
$\sqrt{\text{var}(\hat{W})}$	0.005 42	6×10^{-6}	0.005 42	1×10^{-5}

Table 2. Simulation results (μm) for $u_i = (i - 1)10^\circ, i = 1, 2, \dots, 8$.

	$M = 63, m = 62$		$M = 63.75, m = 61.25$	
	Mean	Sd	Mean	Sd
\hat{W}	125.000	0.015 10	125.013	0.015 10
\bar{w}_8	124.999	0.501 25	125.005	1.253 14
$\sqrt{\text{var}(\hat{W})}$	0.015 16	0.000 15	0.015 17	0.000 37

and $\bar{w}_7 = \sum_{i=1}^7 w_i/7$. The process is repeated 10 000 times. Table 1 lists the statistics of the simulation results for both $(M, m) = (63, 62)$ and $(M, m) = (63.75, 61.25)$.

The row labelled \hat{W} in table 1 displays the mean and standard deviation of the 10 000 simulated \hat{W} . Since the standard error of the random noise is $0.014/\sqrt{7} = 0.005 29$, the estimation method based on the least-squares solution of elliptical parameters contributes insignificantly to the overall uncertainty of the diameter estimate for both $\delta = 0.8\%$ and $\delta = 2\%$. We include the \bar{w}_7 row to compare the uncertainties of \bar{w}_7 obtained by simulation and by (16). The last row shows the mean and standard deviation of the 10 000 estimated standard error of \hat{W} using (18), indicating that (18) is an adequate approximation of $\text{var}(\hat{W})$.

In the second simulation, we employ the same simulation parameters used in the first study except $u_i = (i - 1)10^\circ, i = 1, 2, \dots, 8$. Obviously, this is not a desirable sampling scheme (all the measurements are from the same quadrant), and should be avoided in practice. Table 2 displays the statistics of diameter estimates based on 10 000 simulated samples.

The standard error of the mean horizontal width \bar{w}_8 when $(M, m) = (63, 62)$ in table 2 (0.501 25) is twice as large as the standard error of the mean of eight horizontal widths at random angular orientations (0.250 05 by (15)). With the random-angle scheme, it is likely that the measurements would be drawn from more than one quadrant, resulting in a (relatively) more symmetric distribution of horizontal widths. Table 2 also indicates that \hat{W} is an acceptable diameter estimator even with this poor sampling scheme.

For balanced and complete sampling schemes, the method based on the mean width and the method based on elliptical parameter estimation perform equally well. Tables 3 and 4 display the simulation results for cases with $n = 4$ and 8, and for $(M, m) = (63, 62)$ and $(M, m) = (63.75, 61.25)$.

6. Estimation of diameter with angles subject to error

In real experiments, the angles may be subject to measurement error. In the literature of simple linear regression when both

Table 3. Simulation results (μm) for two balanced schemes when $(M, m) = (63, 62) \mu\text{m}$.

	$n = 4$		$n = 8$	
	Mean	Sd	Mean	Sd
\hat{W}	125.000	0.007 03	125.000	0.004 97
\bar{w}_n	125.002	0.007 03	125.002	0.004 97
$\sqrt{\hat{\text{var}}(\hat{W})}$	0.007 00	4×10^{-9}	0.004 95	2×10^{-9}

Table 4. Simulation results (μm) for two balanced schemes when $(M, m) = (63.75, 61.25) \mu\text{m}$.

	$n = 4$		$n = 8$	
	Mean	Sd	Mean	Sd
\hat{W}	125.012	0.007 03	125.012	0.004 97
\bar{w}_n	125.012	0.007 03	125.012	0.004 97
$\sqrt{\hat{\text{var}}(\hat{W})}$	0.007 00	1×10^{-8}	0.004 95	6×10^{-9}

Table 5. Simulation results (μm) for two sampling schemes with angles subject to error when $(M, m) = (63, 62) \mu\text{m}$.

	$45^\circ (n = 4)$		$10^\circ (n = 8)$	
	Mean	Sd	Mean	Sd
\hat{W}	125.000	0.010 01	125.000	0.021 97
\bar{w}_n	125.002	0.010 01	125.003	0.501 42
$\sqrt{\hat{\text{var}}(\hat{W})}$	0.007 00	6×10^{-9}	0.015 16	0.000 15

variables are subject to measurement errors, it is stated that if the measurement error variance in X (independent variable) is small relative to the variability of the X 's, then errors in the X 's can be safely ignored. If we apply this criterion to our experiments, we would like the angular measurement error variance to be small relative to the variance of the angular measurements. One method of increasing the variance of the angular measurements is to have a balanced sampling scheme. We use simulations to study the effects of angular measurement errors on the second diameter estimation method.

We employ the same simulation parameters used in the previous studies. We allow the orientation u_i to randomly vary within $\pm 1^\circ$ of its nominal value, which represents a worst-case scenario in our experiments. We then generate w_i using the perturbed orientations. The method of elliptical parameter estimation based on nominal u_i and w_i is used to estimate the diameter. Table 5 shows the results for $(M, m) = (63, 62)$.

Table 5 indicates that although the relative increase in the standard error of \hat{W} is large (greater than 40%) when the u_i are subject to error, the absolute increase, however, is not large enough to make \hat{W} unacceptable. It also indicates that errors in the u_i cause $\hat{\text{var}}(\hat{W})$ to underestimate $\text{var}(\hat{W})$.

We replace the ordinary least-squares method with the errors-in-variables method in elliptical parameter estimation. For the case with nominal $u_i = (i - 1)\pi/4$, $i = 1, 2, 3, 4$,

the standard deviation of the 10 000 simulated \hat{W} is found to be 0.009 57, and the mean and standard deviation of the 10 000 simulated $\sqrt{\hat{\text{var}}(\hat{W})}$ are 0.010 64 and 0.001 10, respectively. Thus, the errors-in-variables method produces a closer estimate for the standard error of \hat{W} .

7. Concluding remarks

Geometrically uniform fibres are required in large-scale fibre networks. The optical-fibre industry uses the grey-scale method to measure key fibre geometric parameters. NIST provides SRM fibres so that the industry has artefacts for calibrating their grey-scale systems. The SRM fibres are certified by a contact micrometer that is capable of measuring the cladding diameter accurate to $0.04 \mu\text{m}$. The certified cladding diameter of the SRM fibre is reported in the accompanying certificate.

We proposed a model for diameters measured by the contact micrometer. We presented two methods for estimating the cladding diameter of the SRM fibre. The first estimate is based on the mean of diameter measurements, and requires the measurements to be taken at equally spaced angular orientations. The second estimate is based on the non-linear estimation of elliptical parameters of the model and does not require the special sampling scheme. In preparing SRM fibres, we take measurements at equally spaced angular orientations and use both methods to assure an accurate estimate of the cladding diameter of fibres.

Acknowledgments

This work is a contribution of the NIST and is not subject to copyright in the United States.

References

- [1] Telecommunications Industry Association 1993 *TIA/EIA-455-176 (Fiber Optic Test Procedure FOTP-176): Method for Measuring Optical Fiber Cross-Sectional Geometry by Automated Grey-Scale Analysis* (Arlington, VA: TIA)
- [2] Mechels S E and Young M 1991 *Appl. Opt.* **30** 2202–11
- [3] Young M, Hale P D and Mechels S E 1993 *J. Res. Natl Inst. Stand. Technol.* **98** 203–16
- [4] Fuller W A 1987 *Measurement Error Models* (New York: Wiley)
- [5] Mamileti L, Wang C M, Young M and Vecchia D F 1993 *Appl. Opt.* **31** 4182–5
- [6] Wang C M, Vecchia D F, Matt Y and Brilliant N A 1997 *Technometrics* **39** 25–33
- [7] Young M 1991 *Technical Digest: Optical Fibre Measurement Conference (OFMC), 17–18 September 1991, York* (Teddington, UK: National Physical Laboratory) pp 123–6
- [8] Abramowitz M and Stegun I A 1965 *Handbook of Mathematical Functions (Applied Mathematical Series vol 55)* (Washington DC: US Government Printing Office)
- [9] Wang C M and Lam C T 1997 *Technometrics* **39** 119–26